Available online at www.sciencedirect.com
ScienceDirect
Biochimica et Biophysica Acta 1767 (2007) 686–693
Biochimica et Biophysica Acta
BBA
www.elsevier.com/locate/bbabio

Site-directed mutagenesis on the heme axial-ligands of cytochrome b559 in photosystem II by using cyanobacteria *Synechocystis* PCC 6803

Chung-Hsien Hung, Jing-Yueh Huang, Yi-Fang Chiu, Hsiu-An Chu *

Institute of Plant and Microbial Biology, Academia Sinica, Taipei, Taiwan, 11529, Republic of China

Received 30 September 2006; received in revised form 16 February 2007; accepted 22 February 2007
Available online 3 March 2007

Abstract

Cytochrome (cyt) b559 has been proposed to play an important role in the cyclic electron flow processes that protect photosystem II (PSII) from light-induced damage during photoinhibitory conditions. However, the exact role(s) of cyt b559 in the cyclic electron transfer pathway(s) in PSII remains unclear. To study the exact role(s) of cyt b559, we have constructed a series of site-directed mutants, each carrying a single amino acid substitution of one of the heme axial-ligands, in the cyanobacterium *Synechocystis* sp. PCC6803. In these mutants, His-22 of the α or the β subunit of cyt b559 was replaced with either Met, Glu, Tyr, Lys, Arg, Cys or Gln. On the basis of oxygen-evolution and chlorophyll *a* fluorescence measurements, we found that, among all mutants that were constructed, only the H22Kα mutant grew photoautotrophically, and accumulated stable PSII reaction centers (~81% compared to wild-type cells). In addition, we isolated one pseudorevertant of the H22Yβ mutant that regained the ability to grow photoautotrophically and to assemble stable PSII reaction centers (~79% compared to wild-type cells). On the basis of 77 K fluorescence emission measurements, we found that energy transfer from the phycobilisomes to PSII reaction centers was uncoupled in those cyt b559 mutants that assembled little or no stable PSII. Furthermore, on the basis of immunoblot analyses, we found that in thylakoid membranes of cyt b559 mutants that assembled little or no PSII, the amounts of the D1, D2, cyt b559α and β polypeptides were very low or undetectable but their CP47 and PsaC polypeptides were accumulated to the wild-type level. We also found that the amounts of cyt b559β polypeptide were significantly increased (larger than two folds) in thylakoid membranes of cyt b559 H22YβPS+ mutant cells. We suspected that the increase in the amounts of cyt b559 H22YβPS+ mutant polypeptides in thylakoid membranes might facilitate the assembly of functional PSII in cyt b559 H22YβPS+ mutant cells. Moreover, we found that isolated His-tagged PSII particles from H22Kα mutant cells gave rise to redox-induced optical absorption difference spectra of cyt b559. Therefore, our results concluded that significant fractions of H22Kα mutant PSII particles retained the heme of cyt b559. Finally, this work is the first report of cyt b559 mutants having substitutions of an axial heme-ligands that retain the ability to grow photoautotrophically and to assemble stable PSII reaction centers. These two cyt b559 mutants (H22Kα and H22YβPS+) and their PSII reaction centers will be very suitable for further biophysical and biochemical studies of the functional role(s) of cyt b559 in PSII.

Keywords: Photosystem II; Cytochrome b559; Photoinhibition; Chlorophyll *a* fluorescence; Site-directed mutagenesis; *Synechocystis*

Cytochrome b559 (Cyt b559) is one of the essential components of the photosystem II (PSII) reaction center [1–3]. Cyt b559 is a heme-bridged heterodimer protein that is comprised of α and β subunits (encoded by the *psb*E and *psb*F genes) of 9 and 4 kDa, respectively. In the recent 3.0 Å resolution X-ray crystallographic structural model of PSII, cyt b559 is located on the membrane-facing opening of the Q_B binding pocket [1]. In addition, cyt b559 exhibits different redox potential forms: a high-potential form (HP) with a midpoint redox potential around +400 mV and a low-potential form (LP) with a midpoint redox potential ranging from +200 to

Abbreviations: Chl, chlorophyll *a*; cyt, cytochrome; DCBQ, 2,6-dichloro-p-benzoquinone; DCMU, 3-(3,4-dichloro-phenyl)-1,1-dimethylurea; DM, dodecylmaltoside; Em, erythromycin; EPR, electron paramagnetic resonance; F_{eq}, steady-state fluorescence yield produced by weak monitoring flashes in the presence of DCMU; FTIR, Fourier transform infrared; Gm, gentamycin; HP, the high-potential form of cyt b559; LP, the low-potential form of cyt b559; kDa, kilodaltons; KLH, keyhole limpet hemosyanin; Km, Kanamycin; PCR, polymerase chain reaction; PSII, photosystem II; Pheo, primary pheophitin *a* electron acceptor; Q_A, the primary quinone electron acceptor in PSII; Q_B, the secondary quinone electron acceptor in PSII; wild-type*, control *Synechocystis* strain constructed in the same manner as site-directed mutants, but with no mutation

* Corresponding author. Tel.: +886 2 27899590x308; fax: +886 2 27827954.
E-mail address: chuha@gate.sinica.edu.tw (H.-A. Chu).

0005-2728/$ - see front matter © 2007 Elsevier B.V. All rights reserved.
doi:10.1016/j.bbabio.2007.02.016

+20 mV ([3–6] and reference therein). Despite the recent progress in understanding the structure and function of PSII, the exact role of cyt b559 in PSII is still not clear. The authors of previous studies have proposed that cyt b559 participates in secondary electron transfer pathways that protect PSII from light-induced damage that occurs under photoinhibitory conditions [3,7–12]. In these authors' models, cyt b559 might accept an electron from Q_B [8], plastoquinones [8,9], or Pheophytin (Pheo) [10,11] to prevent the acceptor-side of PSII from generating damaging singlet oxygen species under the acceptor-side photoinhibitory conditions, e.g. the quinone pool is over-reduced and Q_A become double reduced; On the other hand, the high-potential form of cyt b559 might donate its electron to reduce highly oxidized chlorophyll radical species generated in PSII reaction centers under the donor-side photoinhibitory conditions, e.g. the water-splitting reaction is inhibited [3,7].

Previous mutagenesis studies that were performed with *Synechocystis* 6803, *Chlamydomonas reinhardtii* or *Nicotiana tabacum* showed that no stable PSII reaction centers assembled in the absence of either cyt b559 subunit [13–20]. In addition, an early site-directed mutagenesis study that was performed with *Synechocystis 6803* showed that substituting either heme axial ligand (His22 of the α subunit or His22 of the β subunit) with Leu severely diminished the assembly or stability of PSII [19]. Furthermore, another site-directed mutagenesis study that was performed with *C. reinhardtii* showed that the His22Tyr and His22Met mutants of the cyt b559 α subunit were only able to accumulate 10–15% the PSII content of wild-type cells [20]. These *Chlamydomonas* mutants retained significant amounts of oxygen evolution activity. In addition, EPR and optical absorption results on isolated PSII supercomplexes from these cyt b559 mutants showed that their heme-binding pockets of cyt b559 were disrupted. The authors of this work concluded that a redox role for the heme of cyt b559 was not required for oxygen evolution [20].

However, the low PSII contents and disrupted heme-binding pockets of the cyt b559 mutants that were described in the previous studies limit the possibility of employing advanced biophysical methods (e.g. electrochemical, EPR and FTIR measurements) to study the exact role(s) of cyt b559 in the protection of PSII from photoinhibition [4–6,21]. To overcome this problem, we have constructed a series of site-directed mutants of the heme ligands (His-22 of the α subunit and His22 of the β subunit) of cyt b559 by in *Synechocystis* sp. PCC6803. In these mutants, His-22 residue of the α or β subunit of cyt b559 was replaced with Met, Glu, Gln, Tyr, Lys, Arg or Cys. The structural and functional characterizations of the mutant cells and their thylakoid membranes are presented and discussed.

1. Materials and methods

1.1. Growth and preparation of Synechocystis sp. PCC6803 cells

Synechocystis cells were grown in BG-11 medium supplemented with 5 mM glucose. Cultures were propagated at 30 °C under a light intensity of 25–30 μE/m^2/s and were continuously bubbled with sterile, humidified air. For all assays, cells were harvested by centrifugation when their optical density at 730 nm was between 0.7 and 1.2. The optical measurements were performed with a Jasco V-560 UV/VIS spectrophotometer.

1.2. Cloning of psbEFLJ gene cluster DNA fragment

Synechocystis genomic DNA was digested with the restriction enzymes *Hin*dIII and *Eco*RI and the digest was subjected to preparative gel electrophoresis. DNA fragments in the size range 2.0–2.3 kb were excised from the gel and ligated into *Hin*dIII/*Eco*RI-digested pUC119 plasmid, then transformed into *Escherichia coli* (HB101) and selected on solid media containing Amp (100 μg/mL). About 600 Amp^R-transformant colonies were spotted on petri dishes. Southern analysis revealed that two of the transformants contained the desired plasmid (PAC559) bearing the *Hin*dIII/*Eco*RI fragment.

1.3. Construction of plasmids and analysis of nucleotide sequence

The plasmid (PAC559Em^R), used to introduce the desired mutation, was constructed by inserting an Em^R gene cartridge [22] at an *Nhe*I site immediately downstream of the *psb*J gene in the *Hin*dIII/*Eco*RI fragment of the PAC559 plasmid. The plasmid (PAC559Gm^R), used to construct the host strain (Δ*psb*EFLJ), was constructed by replacing the *Acc*I/*Nhe*I fragment within the *Hin*dIII/*Eco*RI fragment of the PAC559 plasmid with a Gm^R gene cartridge [23]. The sequence of oligonucleotides for the desired mutations are listed as the following: H22Cα (5′ C TAC TGG GTG ATC TGC AGC ATC ACC ATC C 3′); H22Eα (5′ T CGC TAC TGG GTC ATC GAA ACC ATC ACC ATC C 3′); H22Kα (5′ TT CGC TAC TGG GTA ATC AAA AGC ATC ACC ATC C 3′); H22Mα (5′ GC TAC TGG GTG ATC ATG AGC ATC ACC ATC C 3′); H22Rα (5′ TAC TGG GTG ATC CGG AGC ATC ACC ATC C 3′); H22Yα (5′ TT CGC TAC TGG GTA ATC TAC AGC ATC ACC ATC C 3′); H22Cβ (5′ GTG CGC TGG CTA GCG GTT TGC ACC CTG GCG G 3′); H22Eβ (5′ GC TGG CTG GCG GTC GAA ACC CTG GCG GTG C 3′); H22Kβ (5′ GTG CGC TGG CTA GCG GTT AAA ACC CTG GCG GTG C 3′); H22Mβ (5′ GC TGG CTG GCG GTC ATG ACC CTG GCG GTG C 3′); H22Qβ (5′ GC TGG CTG GCG GTC CAG ACC CTG GCG GTG C 3′); H22Rβ (5′ TGG CTG GCG GTT CGT ACC CTG GCG GTG C 3′); H22Yβ (5′ GTG CGC TGG CTA GCG GTT TAC ACC CTG GCG G 3′). All the mutants were constructed with a "silent" mutation close to the desired mutation site. These silent mutations introduced or removed convenient sites for restriction endonucleases. The desired mutation was introduced into the plasmid PAC559EM^R by oligonucletide-derived mutagenesis. The mutant strains were constructed by transformation of the desired mutant plasmid into the host strain (Δ*psb*EFLJ). The wild-type* strain was obtained by identical procedures, except that transforming plasmid carried no mutation. Mutants were selected on solid media containing the antibiotic Em (0.1 μg/mL) until their mutated gene was completely segregated. Complete segregation of the mutated gene in these mutant cells was verified by PCR using the B559F (5′-TAGGCGGCTCACAAAATA-3′) and B559R2 (5′-AGCC-CACCTTAAAACCATGATATT-3′) primers. To confirm the identity of each mutant and to verify the absence of undesired mutations, the sequence of the *psb*EFLJ coding region was amplified by PCR using the B559F and B559R (5′-TTACATGGAAGAACCTAA-3′) primers and sequenced. To verify that no mutations outside the *psb*EFLJ coding region contribute to the loss of photoautotrophy in non-photoautotrophic mutants, cells of these mutants were transformed with a cloned fragment of the wild-type gene that included the desired mutation site. In all the mutants tested, photoautotrophic transformants were recovered at frequencies that were far higher than the frequency at which spontaneous photoautotrophic revertants appeared.

1.4. Measurement of photosynthetic oxygen evolution

Concentrated cells were diluted into growth medium held at 25.0 °C in a stirred, water-jacketed cell. 2 mM potassium ferricyanide and 2 mM 2,6-dichloro-p-benzoquinone (DCBQ) were added to the medium immediately prior to the addition of the cells. Steady-state rates of oxygen-evolution were measured with a Clark-type oxygen electrode (YSI model 5331 oxygen probe) fitted with a water-jacketed cell. Saturating illumination was

provided from both sides of the water-jacketed cell by two fiber-optics (Dolan-Jenner model MI 150) illuminators.

1.5. Measurement of chlorophyll a fluorescence at 295 K

Chlorophyll *a* fluorescence measurements at 295 K were performed with a pulse-amplitude-modulation (PAM) fluorimeter (Walz, Germany). Weak monitoring flashes (650 nm) of 1 μs duration were applied at 1.6 kHz. To measure the total yield of variable chlorophyll *a* fluorescence ($F_{max}-F_0$), 26.5 μg chlorophyll cells were incubated with 0.3 mM *p*-benzoquinone and 1 mM ferricyanide in darkness for 5 min. DCMU was then added to a concentration of 40 mM. After another 1 min, hydroxylamine was added to a concentration of 20 mM from a freshly-made 0.5 M stock solution (pH was pre-adjusted to 6.5). The weak monitoring flashes were switched on 20 s after the addition of hydroxylamine and after 1 second later continuous actinic illumination was provided by a Schott (model KL1500) fiber optics illuminator. The difference between the maximum fluorescence produced by the actinic illumination (F_{max}) and the initial fluorescence measure by the monitoring flashes (F_0) was used as a relative measure of the PSII content in mutant cells [24]. Experimental conditions for measurements of the kinetics of charge recombination between Q_A^- and PSII electron donors in response to a saturating flash given to wild-type* and mutant cells in the presence of DCMU are described in the figure legend. Single saturating flashes were provided by a Perkin Elmer (FX-4400) Xenon flash lamp.

1.6. Measurement of fluorescence at 77 K

Fluorescence emission spectra were recorded with a fluorescence spectrometer (Jasco model FP-6500). All the measurements were carried out at 77 K, using cell suspensions at a chlorophyll concentration of 20 μg/mL. The excitation light wavelength used for exciting chlorophyll was 435 nm (Excitation band width 5 nm, Emission band width 1 nm). The excitation light wavelength used for physcoblisomes was 600 nm (Excitation band width 3 nm, Emission band width 1 nm). The spectra are presented in uncorrected form.

1.7. Protein analysis and immunoblotting

Thylakoid membranes were isolated from mid-log phase wild type∗ and mutant cells according to procedures described in ref [25] with the following modifications. 1.2 M betaine and 10% (v/v) glycerol instead of 25% (v/v) glycerol was included in all buffer [26]. Thylakoid membranes (1 μg of Chl) were first removed lipids and chlorophylls and then incubated in 30 μL denaturing buffer at 37 °C for 1 h prior to 18% or 24% SDS-PAGE with 6 M urea [27]. For the detection of D1 or D2 polypeptides, rabbit antisera specific to the D1 and D2 polypeptides were used as the primary antibody and alkaline phosphatase-conjugated goat anti rabbit immuno-globulin G antibody was used as the secondary antibody (Promega). Protein bands were visualized by a colorimetric reaction using BCIP-NBT system (Sigma). D1 antibodies were raised in rabbits against an OVA-conjugated synthetic polypeptide that carried the 225–249 amino acid sequence (on the DE loop) of the D1 polypeptide of *Synechocystis* 6803. D2 antibodies were raised in rabbits against an OVA-conjugated synthetic polypeptide that carried the 219–241 amino acid sequence (on the DE loop) of the D2 polypeptide of *Synechocystis* 6803. Cyt b559α polypeptide antibodies were raised in rabbits against an KLH-conjugated synthetic polypeptide that carried the 1–17 amino acid sequence of the cyt b559α polypeptide of *Synechocystis* 6803. CP47 and PsaC antibodies were purchased from Agrisera.

1.8. Reduced minus oxidized difference spectra of cyt b559 in wild-type and mutant PSII particles

Oxygen-evolving His-tagged PSII particles were isolated by Ni-NTA affinity chromatography from wild-type* and H22Kα mutant cells which contain a His-tag on their CP47 proteins as described in reference [26]. The oxygen activity for wild-type* and H22Kα mutant PSII particles were about 2100 and 1160 μmol of O_2/mg of Chl per hour, respectively. Tris-washed samples were prepared by 30 min incubation of oxygen-evolving PSII particles (0.5 mg of Chl/mL) in a buffer containing 1 M Tris (pH 8.0) and 1.25 M EDTA in the room light on ice. Samples were then mixed with the same volume of 20% PEG8000 and centrifuged at 48,000×*g* for 30 min. The pellets were re-suspended with a small volume of buffer [50 mM Mes, 5 mM $MgCl_2$, 20 mM $CaCl_2$, 10% glycerol, 1.2 M betaine, 0.03% (W/V) DM, pH 6.0] and finally stored at −80 °C until use. Optical absorption difference measurements were performed on suspensions of wild-type* and mutant PSII particles (20 μg/ml Chl) in 1 ml MMNB buffer (25 mM Mes, 5 mM $MgCl_2$, 10 mM NaCl, 1 M betaine, 0.03% DM, pH 5.7) at the room temperature on a Jasco V-560 UV/VIS spectrophotometer with band width 1.0 nm. The sample suspension was oxidized by adding 0.1 mM $K_3Fe(CN)_6$ (from a fresh made 10 mM stock solution) and the spectrum was recorded and stored as the oxidized spectrum (the baseline). A few grains of $Na_2S_2O_4$ were then added to complete reduction of cyt b559 and the reduced spectrum was recorded.

2. Results

2.1. Growth, oxygen-evolution characteristics, and PSII contents of mutant cells

The growth characteristics, light-saturated oxygen-evolution activity, and PSII contents of the mutant strains that are discussed in this study are listed in Table 1. Most mutant strains were obligate photoheterotrophs, requiring 5 mM glucose for propagation. The exceptions were H22Kα and H22YβPS+ (pseudorevertant), both of which could grow photoautotrophically. Originally, H22Yβ mutant cells could not grow photoautotrophically and could not assemble stable PSII reaction centers. However, one photoautotrophic "revertant" of H22Yβ was identified. The DNA sequence of the coding region of the *psb*EFLJ genes in this H22YβPS+ mutant strain showed that the "revertant" strain retained both the H22Yβ mutation and the silent mutation that was introduced to create a new *Nhe*I restriction site. However, no additional mutations were identified within the coding regions of the *psb*EFLJ genes. Therefore, we conclude that a second-site mutation is located elsewhere on the genome of the H22YβPS+ revertant strain. Currently we are in the process of identifying the location of this second site-mutation.

Table 1
Summary of properties of cyt b559 mutant cells

Mutation strain	PS growth	O_2 evolution (% of wild type*)	PSII content (% of wild type*)
wild-type*	+	100±20	100±15
H22Kα	+	49±12	81±16
H22Kβ	−	14±5	23±12
H22Yα	−	0–5	17±3
H22YβPS+	+	43±24	79±19
H22Yβ	−	0–6	13±7
H22Cα	−	~4	15±8
H22Cβ	−	~0	13±5
H22Rα	−	~4	4±1
H22Rβ	−	0	0
H22Eα	−	0	0
H22Eβ	−	0	~0
H22Mα	−	~0	3±2
H22Mβ	−	~0	25±3
H22Qβ	−	0	0

Experimental conditions are described in Materials and methods. The average O_2 evolution rate of wild-type* cells was 440±87 μmol O_2/mg Chl×h. The average variable fluorescence yield of wild-type* cells was 0.39±0.06.

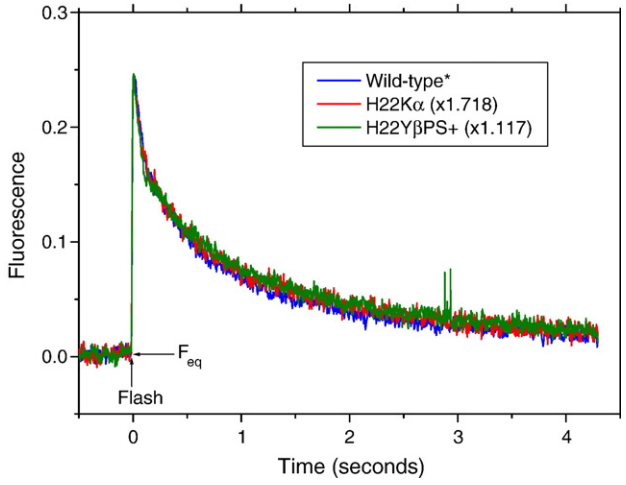

Fig. 1. The kinetics of charge recombination between Q_A^- and PSII electron donors in response to a saturating flash given to wild-type* (Blue trace), H22Kα(Red trace) and H22YβPS+ cells (Green trace) in the presence of DCMU by chlorophyll *a* fluorescence measurement. Conditions: 26.5 μg of Chl in 1 mL of 50 mM MES-NaOH, 25 mM $CaCl_2$, 10 mM NaCl, pH 6.5. Samples were incubated in darkness for 1 min in the presence of 0.3 mM *p*-benzoquinone and 1 mM potassium ferricyanide before DCMU was added to the final concentration of 40 μM.

Under our experimental growth conditions for photoautotrophic growth (light intensity of 25–30 μE/m^2/s), the doubling times for the wild-type*, H22Kα and H22YβPS+ cells were 13.2, 13.7 and 25.9 h, respectively. Under high-light growth conditions for photoautotrophic growth (light intensity of 80–90 μE/m^2/s), the doubling times for the wild-type* and H22Kα cells increased to 8.9 and 11.5 h, respectively. However, H22YβPS+ cells failed to grow under these high-light growth conditions, presumably because of light-induced damage caused by photoinhibition. On the basis of the total yield of variable chlorophyll *a* fluorescence ($F_{max}-F_0$) at constant chlorophyll concentration, H22Kα and H22YβPS+ mutant cells contained ~80% PSII content of wild-type* cells (see Table 1). In contrast, the other cyt b559 mutant cells contained only 0–25% PSII content of wild-type* cells. Furthermore, H22Kα and H22YβPS+ cells showed light-saturated oxygen-evolution rates of 40–50% compared to wild-type* cells. Among the mutant cells that could not grow photoautotrophically, H22Kβ cells showed the highest light-saturated oxygen-evolution rate (~14% compared to wild-type* cells), whereas the other mutant cells only showed rates of 0–6% compared to wild-type* cells (see Table 1). Oxygen-evolution rates of thylakoid membranes from wild-type*, H22YβPS+ and H22Kα cyt b559 cells were 203±2, 78±22 and 85±25 μmol O_2/mg Chl×h, respectively. Thylakoid membranes from H22Yβ, H22Yα, H22Kβ, and Δ*psb*EFLJ mutant cells did not have detectable oxygen-evolution activity.

2.2. Charge recombination between Q_A^- and PSII electron donors

The kinetics of charge recombination between Q_A^- and PSII electron donors is sensitive to the presence or absence of photooxidizable Mn ion and the redox potential of Q_A^- in PSII [24,28]. In addition, the yield of variable chlorophyll *a* fluorescence is believed to be proportional to the concentration of Q_A^- in *Synechocystis* 6803 [24]. Fig. 1 shows the kinetics of charge recombination between Q_A^- and PSII electron donors in response to a saturating flash given to wild-type*, H22Kα and H22YβPS+ cells in the presence of DCMU as measured by chlorophyll *a* fluorescence. Both H22Kα and H22YβPS+ cells showed very similar kinetics of charge recombination compared to that of wild-type cells. These results suggest that the Mn cluster and Q_A are intact in PSII of H22Kα and H22YβPS+ cells. Furthermore, the flash-induced yields of variable chlorophyll *a* fluorescence in H22Kα and H22YβPS+ cells were 1.7 and 1.1 fold lower than that of wild-type* cells (see Fig. 1). These lowered yields roughly correlated with the lower estimated PSII contents in the mutants (Table 1).

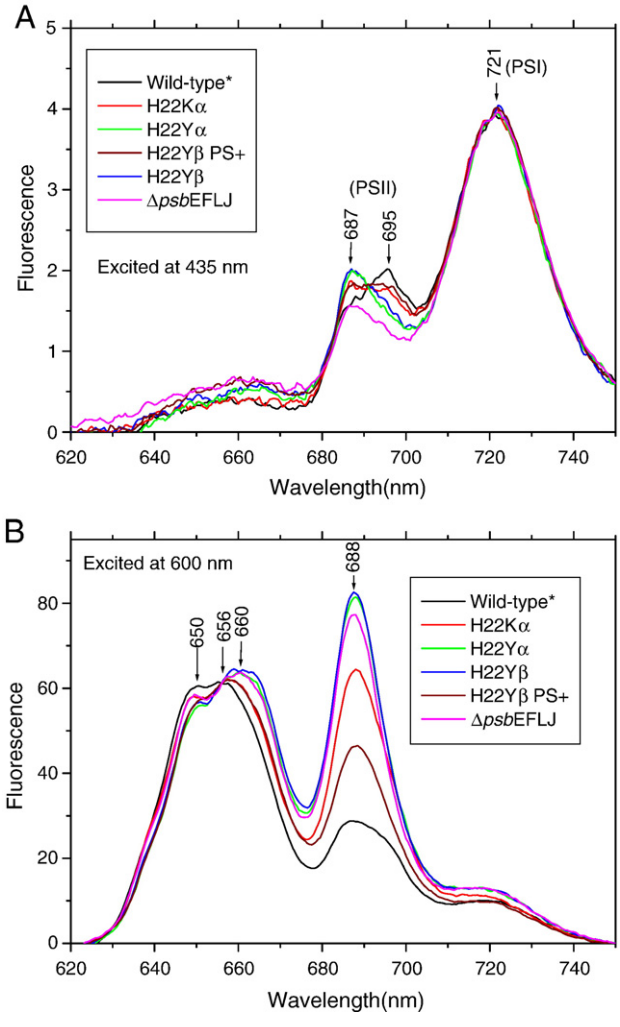

Fig. 2. 77K-fluorescence emission spectra from wild-type* and cyt b559 mutant cells. (A) Excited chlorophyll at 435 nm (Excitation band width 5 nm; emission band width 1 nm; spectra were normalized at 721 nm) and (B) excited phycobilisomes at 600 nm (Excitation band width 3 nm; Emission band width 1 nm; spectra were normalized at 656 nm). All the measurements were carried out at 77 K, using cell suspensions at a chlorophyll concentration of 20 μg/mL.

2.3. 77 K fluorescence emission spectra

Fig. 2 shows the fluorescence emission spectra of intact wild type and cyt b559 mutant cells at 77 K. In wild-type*, H22Kα and H22YβPS+ cells, preferential excitation of chlorophyll at 435 nm resulted in three emission peaks, at ~687, ~695 and ~721 nm. According to previous studies, emission peaks at ~687 and ~695 nm originate from Chl *a* in PSII, whereas the emission peak at ~721 nm originates from Chl *a* in PSI ([14, 29] and reference therein). In contrast, the cyt b559 mutants that contained little or no detectable PSII reaction centers (H22Yα, H22Yβ and Δ*psb*EFLJ) lacked an emission peak at ~695 nm, although the emission peaks at ~687 and ~721 nm were present. The origin of the emission peak at ~695 nm has been suggested to originate from CP47 functionally coupled to the PSII reaction center [14]. Therefore, the absence the emission peak at ~695 nm in these cyt b559 mutant strains (H22Yα, H22Yβ and Δ*psb*EFLJ) is correlated with their low PSII contents (see Table 1). In addition, the emission peak at ~687 nm has been suggested to originate primarily from CP43 in intact cyanobacterial cells [14,30,31]. This peak was detected in all of the cyt b559 mutants, indicating that the CP43 polypeptide was not only present but that it binds chlorophyll in the absence of PSII reaction centers in these mutants. We cannot discard that part of the 687 nm fluorescence is related to disconnected phycobilisomes in H22Yα, H22Yβ and Δ*psb*EFLJ mutants.

To determine if there was energy transfer from physcobilisomes to the PSII reaction centers in the cyt b559 mutants, the fluorescence emission spectra were recorded from cells that were excited at 600 nm, where the phycobilin pigments preferentially absorb. If the energy transfer from phycobilisomes to PSII reaction center is inhibited, a characteristic fluorescence emission from individual pigments in phycobilisomes or PSII will be observed at 77 K. As shown in Fig. 2B, the 77 K fluorescence emission spectra of wild-type cells showed a fluorescence peak at ~656 nm arising from allophycocyanin and a peak at ~650 nm arising from phycocyanins ([29] and references therein). In the spectra of the cyt b559 mutant cells, the peak at ~650 nm (arising from phycocyanins) is present but the peak at ~656 nm (arising from allophycocyanin) appears shifted to ~660 nm. This spectral shift indicates that some structural changes might have occurred in allophycocyanin that affected its fluorescence characteristics in the cyt b559 mutants. In addition, 77 K fluorescence spectra from mutant cells that contain little or no PSII reaction centers (H22Yα, H22Yβ and Δ*psb*EFLJ) showed a strongly enhanced emission peak at ~688 nm compared to spectra of wild-type*, H22Kα and H22YβPS+ cells. The emission peak at ~688 nm originates from terminal phycobilin emitters or from CP43 ([14,29–31] and reference therein). Therefore, the strong enhancement of the emission peak at ~688 nm in H22Yα, H22Yβ and Δ*psb*EFLJ cells indicates that the energy transfer from phycobilisomes to PSII reaction centers has been uncoupled in these cyt b559 mutants because of a lack of assembled PSII. The emission peak at ~688 nm was also significantly enhanced in the 77 K fluorescence spectra of H22Kα and H22YβPS+ cells compared to the wild-type* spectrum, but its intensity was significantly lower than spectra of H22Yα, H22Yβ and Δ*psb*EFLJ cells. Our results suggest that the energy transfer from phycobilisome to PSII reaction centers were partially inhibited or uncoupled in H22Kα and H22YβPS+ cells.

2.4. Immunoblot analysis

To detect the presence of photosystem II and photosystem I polypeptides in thylakoid membranes purified from the wild-type* and cyt b559 mutant cells, immunoblot analyses were

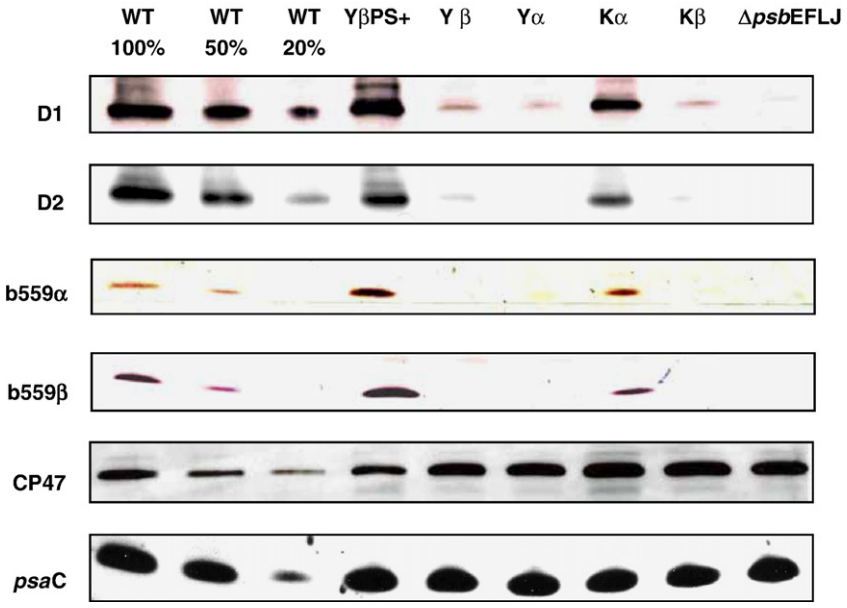

Fig. 3. Immunoblot analysis of D1, D2, cyt b559α, cyt b559β, CP47 and *psa*C proteins in wild-type* and cyt b559 mutant thylakoid membranes. Intact thylakoid membranes from wild-type*, H22YβPS+, H22Yβ, H22Yα, H22Kα, H22Kβ, and Δ*psb*EFLJ cells were subjected to denaturing sodium dodecyl sulphate/polyacrylamide gel electrophoresis, transferred to nitrocellulose filters and immunostained with antibodies raised against the selected polypeptide.

performed with antibodies directed against D1, D2, cyt b559α, cyt b559β, CP47 and *psa*C polypeptides as shown in Fig. 3. Antibodies recognized the D1 D2, cyt b559α, and cyt b559β polypeptide bands in membrane fractions of wild-type*, H22Kα and H22YβPS+ cells. In contrast, the presence of D1 polypeptide was barely detectable (less than 10% compared to wild-type*) or undetectable in the membrane fraction from H22Yα, H22Yβ and H22Kβ cells and was undetectable in those of Δ*psb*EFLJ cells. Our immunoblot results clearly show that the amount of D1, D2, cyt b559α and β polypeptides are very low or undetectable in thylakoid membranes purified from those cyt b559 mutants that contain little or no PSII content. In contrast, CP47 and PsaC polypeptides were detected in all mutant thylakoid membranes and accumulated comparable to the wild-type level. Furthermore, we also found that the amounts of cyt b559β polypeptide were significantly increased (larger than 2 fold compared to wild-type*) in thylakoid membranes of cyt b559 H22YβPS+ mutant cells.

2.5. Redox-induced optical absorption difference spectra of the cyt b559 heme

To facilitate the isolation of PSII particles, we constructed wild-type* and H22Kα mutant strains that contain a hexahistidine-tag (His-tag) fused to the C-terminus of CP47 (26). The dithionite-reduced minus ferricyanide-oxidized difference spectra of the cyt b559 heme in His-tagged PSII particles isolated from wild-type* and H22Kα mutant cells were shown in Fig. 4. Both wild-type* (green trace) and H22Kα mutant PSII particles (red trace) gave rise to dithionite-reduced minus ferricyanide-oxidized difference spectra that can be attributed to redox-induced absorption changes of cyt b559 and cyt c550. On the other hand, difference spectra from Tris-washed wild-type* (magenta trace) and H22Kα mutant PSII particles (blue trace) [that were depleted of Mn ions and extrinsic polypeptides (including cyt c550)] showed the maximum of absorption at around 559.5 nm that can be attributed to redox-induced absorption changes of cyt b559. In addition, our results in Fig. 4 showed that the amplitude of the absorption of cyt b559 in H22Kα mutant PSII particles are about the one third of the absorption of cyt b559 in wild-type* PSII particles. On the basis of the above results, we concluded that significant fractions of H22Kα mutant PSII particles retained the heme of cyt b559. Furthermore, our results also showed that the change in the coordination of the cyt b559 heme in Tris-washed H22Kα mutant PSII particles did not significantly modify the maximum absorption of cyt b559 (in Fig. 4, blue trace). Currently we are in the progress of applying electrochemical redox-titration measurement to determine the redox potential of cyt b559 and also the proportion between LP and HP changes in H22Kα mutant PSII particles in comparison with those in wild-type* PSII particles.

3. Discussion

Previous site-directed mutagenesis studies performed with the cyanobacterium *Synechocystis 6803* or the green algae

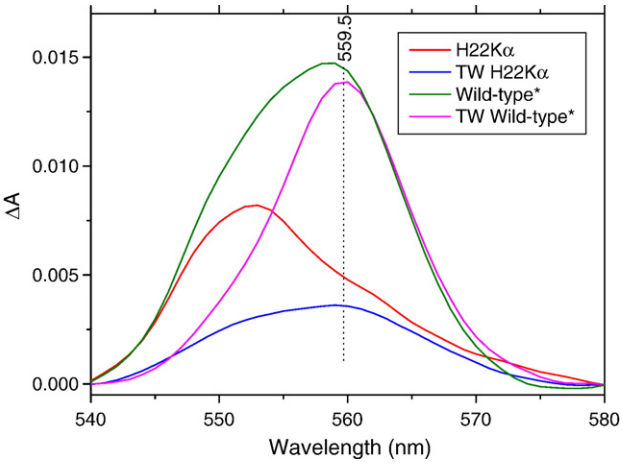

Fig. 4. The dithionite-reduced minus ferricyanide-oxidized difference spectra of cyt b559 heme in wild-type* and H22Kα mutant PSII particles. Spectra of untreated wild-type* and H22Kα mutant PSII particles are in green and red colors, respectively; Spectra of Tris-washed (TW) wild-type* and H22Kα mutant PSII particles are in magenta and blue colors, respectively. All the measurements were performed at the room temperature.

Chlamydomonas have shown that site-directed mutations of the heme axial-ligands (His22) of cyt b559 severely affect the assembly of PSII [19,20]. One of the major objectives of this work was to find site-directed mutants of the axial ligands (His22) of cyt b559 in PSII that retain the heme of cyt b559 and accumulation of stable PSII reaction centers. Among all the mutants that were constructed (Table 1), H22Kα and H22YβPS+ (pseudorevertant) were able to assemble stable PSII reaction centers (up to ~80% compared to wild-type) and to grow photoautotrophically. Our chlorophyll *a* fluorescence results (see Fig. 2) also indicate that the Mn cluster and Q_A are intact in H22Kα and H22YβPS+ cells. In addition, our result in Fig. 4 showed that H22Kα mutant PSII particles gave rise to redox-induced optical absorption difference spectra of cyt b559. Therefore, our result concluded that significant fractions of H22Kα mutant PSII particles retained the heme of cyt b559. On the basis of the above results, H22Kα and H22YβPS+ cells would be very suitable for further biophysical and biochemical studies on the functional role(s) of cyt b559 in protecting PSII against light-induced damage under photoinhibitory conditions.

On the basis of immunoblot analyses in Fig. 3, we found that the amounts of D1, D2, cyt b559α and β polypeptides were very low or undetectable in thylakoid membranes of cyt b559 mutants that assembled little or no PSII but the amounts of CP47 and PsaC polypeptides were accumulated to the wild-type level. Our results showed that most cyt b559 mutants were unable to assemble stable PSII reaction centers or to grow photoautotrophically. Therefore, our results are consistent with previous mutant studies that substitutions of the heme axial-ligands (His22) of cyt b559 severely impact the assembly or stability of PSII [19,20]. In addition, our result and also results from the previous study showed that CP47 accumulated in the thylakoid membrane of *Synechocystis* 6803 in the absence of D1, D2, cyt b559α and β polypeptides. In contrast, a previous study showed that CP47 were unable to accumulate in the

thylakoid membrane of *psb*E null mutant of *Chlamydomonas* [16]. They attributed the more drastic effect seen in *Chlamydomonas* mutants to a more efficient proteolytic system in the chloroplast for the removal of mis-assembled PSII complex [16]. Furthermore, we found that the amounts of the cyt b559 β polypeptides were significantly increased in thylakoid membranes of cyt b559 H22YβPS+ mutant cells compared to wild-type* cells. We suspected that the increase in the amounts of cyt b559 H22YβPS+ mutant polypeptides in thylakoid membranes might facilitate the assembly of functional PSII in cyt b559 H22YβPS+ mutant cells. We are in the process of testing this proposal.

On the basis of our finding that H22Kα cells grow photoautotrophically and assemble stable PSII reaction centers (up to ~80% compared to wild-type) and that H22Kβ cells demonstrate the highest light-saturated rates of oxygen-evolution (~14% compared to wild-type*) among the mutants that fail to grow photoautotrophically, we propose that Lys is able to replace His 22 on the α subunit and to partly replace His 22 on the β subunit of cyt b559 as the heme iron axial ligand. To our knowledge, there are very few examples of lysine-histidine heme ligation in cytochromes [32,33]. Therefore, the H22Kα and H22Kβ mutants should prove valuable for structural studies of lysine-histidine ligation in cytochromes.

The authors of previous studies have proposed that different redox-potential forms of cyt b559 are involved in cyclic electron transfer pathways that protect PSII from light-induced damage under both acceptor-side and donor-side photoinhibitory conditions [3,7–11]. Because H22Kα and H22YβPS+ cells are able to grow photoautotrophically and assemble stable PSII reaction centers, presumably these mutants preserve the hydrophobic heme environment of cyt b559 in stabilizing the structure of the PSII reaction center. It will be very interesting to determine the redox potentials of cyt b559 in PSII particles isolated from H22Kα and H22YβPS+ cells and to determine how the redox potential of cyt b559 influences its function in protecting PSII against light-induced damage.

4. Conclusions

In this study, we identified two cyt b559 mutant strains, H22Kα and H22YβPS+, that assemble stable PSII reaction centers and grow photoautotrophically. These two mutant strains and their PSII particles will facilitate further biophysical and biochemical studies designed to determine the exact role(s) of cyt b559 in the protection of PSII against light-induced damage under photoinhibitory conditions.

Acknowledgments

We are grateful to Dr. Richard J. Debus for generous gifts of the cyt b559 mutant strains of *Synechocystis* 6803 and for critical reading of this manuscript. We thank Dr. Josef Komenda for providing antibodies against the residues 2–12 of the cyt b559β polypeptide of *Synechocystis* 6803. We are also indebted to the reviewers for helpful comments on the manuscript.

This work was supported by Academia Sinica to H.A.C.

References

[1] B. Loll, J. Kern, W. Saenger, A. Zouni, J. Biesiadka, Towards complete cofactor arrangement in the 3.0 Å resolution structure of photosystem II, Nature 438 (2005) 1040–1044.
[2] K.N. Ferreira, T.M. Iverson, K. Maghlaoui, J. Barber, S. Iwata, Architecture of the photosynthetic oxygen-evolving center, Science 303 (2004) 1831–1838.
[3] D.H. Stewart, G.W. Brudvig, Cytochrome b559 of photosystem II, Biochim. Biophys. Acta 1367 (1998) 63–87.
[4] L.K. Thompson, A.-F. Miller, C.A. Buser, J.C. de Paula, G.W. Brudvig, Characterization of the multiple forms of cytochrome b559 in photosystem II, Biochemistry 28 (1989) 8048–8056.
[5] M. Roncel, J.M. Ortega, M. Losada, Factors determining the special redox properties of photosynthetic cytochrome b559, Eur. J. Biochem. 268 (2001) 4961–4968.
[6] M. Roncel, A. Boussac, J.L. Zurita, H. Bottin, M. Sugiura, D. Kirilovsky, J.M. Ortega, Redox properties of the photosystem II cytochrome b559 and c550 in the cyanobacterium *Thermosynechococcus elongates*, J. Biol. Inorg. Chem. 8 (2003) 206–216.
[7] L.K. Thompson, G.W. Brudvig, Cytochrome b-559 may function to protect photosystem II from photoinhibition, Biochemistry 27 (1988) 6653–6658.
[8] C.A. Buser, B.A. Diner, G.W. Brudvig, Photooxidation of cytochrome b559 in oxygen-evolving photosystem II, Biochemistry 31 (1992) 11449–11459.
[9] N. Bondarava, L. De Pascalis, S. Al-Babili, C. Goussias, J.R. Golecki, P. Beyer, R. Bock, A. Krieger-Liszkay, Evidence that cytochrome b559 mediates the oxidization of reduced plastoquinone in the dark, J. Biol. Chem. 278 (2003) 13554–13560.
[10] L. Nedbal, G. Samson, J. Whitmarsh, Redox state of a one-electron component controls the rate of photoinhibition of photosystem II, Proc. Natl. Acad. Sci. U. S. A. 89 (1992) 7929–7933.
[11] J. Barber, J. De Las Rivas, A functional model for the role of cytochrome b_{559} in the protection against donor and acceptor side photoinhibition, Proc. Natl. Acad. Sci. U. S. A. 90 (1993) 10942–10946.
[12] E.-M. Aro, I. Virgin, B. Andersson, Photoinhibition of photosystem II. Inactivation, protein damage and turnover, Biochim. Biophys. Acta 1143 (1993) 113–134.
[13] H.B. Pakrasi, J.G.K. Williams, C.J. Arntzen, Targeted mutagenesis of the *psbE* and *psbF* genes blocks photosynthetic electron transport: evidence for a functional role of cytochrome b559 in photosystem II, EMBO J. 7 (1988) 325–332.
[14] H.B. Pakrasi, B.A. Diner, J.G.K. Williams, C.J. Arntzen, Deletion mutagenesis of the cytochrome b559 protein inactivates the reaction center of photosystem II, Plant Cell 1 (1989) 591–597.
[15] H.B. Pakrasi, K.J. Nyhus, H. Granok, Targeted deletion mutagenesis of the β subunit of cytochrome b559 protein destabilizes the reaction center of photosystem II, Z. Naturforsch. 45c (1990) 423–429.
[16] F. Morais, J. Barber, P.J. Nixon, The chloroplast-encoded α subunit of cytochrome b559 is required for assembly of the photosystem two complex in both the light and the dark in *Chlamydomonas reinhardtii*, J. Biol. Chem. 273 (1998) 29315–29320.
[17] M. Swiatek, R.E. Regel, J. Meurer, G. Wanner, H.B. Pakrasi, I. Ohad, R.G. Herrmann, Effects of selective inactivation of individual genes for low-molecular-mass subunits on the assembly of photosystem II, as revealed by chloroplast transformation: the *psbEFLJ* operon in *Nicotiana tabacum*, Mol. Gen. Genomics 268 (2003) 699–710.
[18] M. Suorsa, R.E. Regel, V. Paakkarinen, N. Battchikova, R.G. Herrmann, E.-M. Aro, Protein assembly of photosystem II and accumulation of subcomplexes in the absence of low molecular mass subunits PsbL and PsbJ, Eur. J. Biochem. 271 (2004) 96–107.
[19] H.B. Pakrasi, P. De Ciechi, J. Whitmarsh, Site directed mutagenesis of the heme axial ligands of cytochrome b559 affects the stability of the photosystem II complex, EMBO J. 10 (1991) 1619–1627.
[20] F. Morais, K. Kühn, D.H. Stewart, J. Barber, G.W. Brudvig, P.J. Nixon, Photosynthetic water oxidation in cytochrome b559 mutants containing a disrupted heme-binding pocket, J. Biol. Chem. 276 (2001) 31986–31993.

[21] C. Berthomieu, A. Boussac, W. Mäntele, J. Breton, E. Nabedryk, Molecular changes following oxidoreduction of cytochrome b559 characterized by Fourier transform infrared difference spectroscopy and electron paramagnetic resonance, Biochemistry 31 (1992) 11460–11471.
[22] J. Elhai, C.P. Wolk, A versatile class of positive-selection vectors based on the nonviability of palindrome-containing plasmids that allows cloning into long polylinkers, Gene 68 (1988) 119–138.
[23] J.C.P. Yin, M.P. Krebs, W.S. Reznikoff, Effect of dam methylation on Tn5 transposition, J. Mol. Biol. 199 (1988) 33–45.
[24] H.-A. Chu, A.P. Nguyen, R.J. Debus, Site-directed photosystem II mutants with perturbed oxygen-evolving properties: 1. Instability or inefficient assembly of the manganese cluster *in vivo*, Biochemistry 33 (1994) 6137–6149.
[25] X.-S. Tang, B.A. Diner, Biochemical and spectroscopic characterization of a new oxygen-evolving photosystem II core complex from the cyanobacterium *Synechocystis* PCC 6803, Biochemistry 33 (1994) 4594–4603.
[26] M.A. Strickler, L.M. Walker, W. Hillier, R.J. Debus, Evidence from biosynthetically incorporated strontium and FTIR difference spectroscopy that the C-terminus of the D1 polypeptide of photosystem II does not ligate calcium, Biochemistry 44 (2005) 8571–8577.
[27] Y. Kashino, H. Koike, K. Satoh, An improved sodium dodecyl sulfate-polyacrylamide gel electrophoresis system for the analysis of membrane protein complexes, Electrophoresis 22 (2001) 1004–1007.
[28] P.J. Nixon, B.A. Diner, Aspartate 170 of the photosystem II reaction center polypeptide D1 is involved in the assembly of the oxygen-evolving manganese cluster, Biochemistry 31 (1992) 942–948.
[29] G. Ajlani, C. Vernotte, L. DiMagno, R. Haselkorn, Physobilisome core mutants of *Synechocystis* PCC 6803, Biochim. Biophys. Acta 1231 (1995) 189–196.
[30] V.A. Dzelzkalns, L. Bogorad, Spectral properties and composition of reaction center and ancillary polypeptide complexes of photosystem II deficient mutants of *Synechocystis* 6803, Plant Physiol. 90 (1989) 617–623.
[31] G. Ajlani, C. Vernotte, Construction of a phycobiliprotein-less mutant of *Synechocystis* sp. PCC 6803, Plant Mol. Biol. 37 (1998) 577–580.
[32] J. Li, E. Darrouzet, I.K. Dhawan, M.K. Johnson, A. Osyczka, F. Daldal, D.B. Knaff, Spectroscopic and oxidation-reduction properties of *Rhodobacter capsulatus* cytochrome *c*1 and its M183K and M183H variants, Biochim. Biophys. Acta 1556 (2002) 175–186.
[33] M. Ubbink, A.P. Campos, M. Teixeira, N.I. Hunt, A.O. Hill, G.W. Canters, Characterization of mutant Met100Lys of cytochrome *c*-550 from *Thiobacillus versutus* with lysine-histidine heme ligation, Biochemistry 33 (1994) 10051–10059.